



Conduction band offset in the $\text{Al}_x\text{Ga}_{1-x-y}\text{In}_y\text{P}/\text{Ga}_{0.52}\text{In}_{0.48}\text{P}$ system as studied by luminescence spectroscopy

D. Vignaud, F. Mollot

► To cite this version:

D. Vignaud, F. Mollot. Conduction band offset in the $\text{Al}_x\text{Ga}_{1-x-y}\text{In}_y\text{P}/\text{Ga}_{0.52}\text{In}_{0.48}\text{P}$ system as studied by luminescence spectroscopy. *Journal of Applied Physics*, 2003, 93 (1), pp.384. 10.1063/1.1528309 . hal-00018496

HAL Id: hal-00018496

<https://hal.science/hal-00018496>

Submitted on 25 May 2022

HAL is a multi-disciplinary open access archive for the deposit and dissemination of scientific research documents, whether they are published or not. The documents may come from teaching and research institutions in France or abroad, or from public or private research centers.

L'archive ouverte pluridisciplinaire **HAL**, est destinée au dépôt et à la diffusion de documents scientifiques de niveau recherche, publiés ou non, émanant des établissements d'enseignement et de recherche français ou étrangers, des laboratoires publics ou privés.

Conduction band offset in the $\text{Al}_x\text{Ga}_y\text{In}_{1-x-y}\text{P}/\text{Ga}_{0.52}\text{In}_{0.48}\text{P}$ system as studied by luminescence spectroscopy

Cite as: Journal of Applied Physics **93**, 384 (2003); <https://doi.org/10.1063/1.1528309>

Submitted: 05 July 2002 • Accepted: 21 October 2002 • Published Online: 23 December 2002

D. Vignaud and F. Mollot



View Online



Export Citation

ARTICLES YOU MAY BE INTERESTED IN

[Band parameters for III-V compound semiconductors and their alloys](#)

Journal of Applied Physics **89**, 5815 (2001); <https://doi.org/10.1063/1.1368156>

[Band offsets at GaInP/AlGaInP\(001\) heterostructures lattice matched to GaAs](#)

Applied Physics Letters **73**, 1098 (1998); <https://doi.org/10.1063/1.122096>

[Determination of the GaInP/AlGaInP band offset](#)

Applied Physics Letters **57**, 2698 (1990); <https://doi.org/10.1063/1.104193>

Lock-in Amplifiers
up to 600 MHz



Zurich
Instruments



Conduction band offset in the $\text{Al}_x\text{Ga}_y\text{In}_{1-x-y}\text{P}/\text{Ga}_{0.52}\text{In}_{0.48}\text{P}$ system as studied by luminescence spectroscopy

D. Vignaud^{a)} and F. Molloy

*Institut d'Electronique, de Microélectronique et de Nanotechnologie (IEMN, UMR CNRS 8520),
Av. Poincaré, P. O. Box 69, 59652 Villeneuve d'Ascq Cedex, France*

(Received 5 July 2002; accepted 21 October 2002)

The conduction band offset ΔE_c between the lattice-matched, compressively, or tensilely strained $\text{Al}_x\text{Ga}_y\text{In}_{1-x-y}\text{P}$ and $\text{Ga}_{0.52}\text{In}_{0.48}\text{P}$, grown on GaAs, has been measured by combined photoluminescence and photoluminescence excitation spectroscopy at 10 K. The goal was to study the composition of the quaternary barrier for which the maximum offset ΔE_c is reached in such heterostructures. Within the limited set of barrier composition studied here, the optimum material for this purpose is the lattice-matched $\text{Al}_{0.31}\text{Ga}_{0.21}\text{In}_{0.48}\text{P}$, for which $\Delta E_c = 210 \pm 15$ meV. Comparison with calculations based on the model solid theory allows one to precisely measure the parameters involved in this model, although a precise determination of all the deformation potentials is out of reach with the limited set of results presented here. Nevertheless, estimations using this set of parameters suggest that strained $\text{Al}_x\text{Ga}_y\text{In}_{1-x-y}\text{P}$ cannot improve the conduction offset compared to the strain-free material. © 2003 American Institute of Physics. [DOI: 10.1063/1.1528309]

I. INTRODUCTION

Some device applications, such as the high electron mobility transistors, require a material acting as an electron barrier, with the highest possible conduction band offset (CBO) relative to the channel layer. For example, some of these devices involve a strained $\text{In}_{0.2}\text{Ga}_{0.8}\text{As}$ well when grown on a GaAs substrate. Many barrier materials have been tested in this case: the quaternary $\text{Al}_x\text{Ga}_y\text{In}_{1-x-y}\text{P}$ (AlGaInP for short, in the following) seems to be one of the best choices to get the highest CBO.¹⁻³ Up until now, the quaternary lattice matched on GaAs, that is $(\text{Al}_z\text{Ga}_{1-z})_{0.52}\text{In}_{0.48}\text{P}$, has been mainly studied.⁴⁻¹⁴ The best composition, regarding the CBO, is around $z=0.6$ ($\text{Al}_{0.31}\text{Ga}_{0.21}\text{In}_{0.48}\text{P}$), the one for which the Γ and X minima are degenerated.¹⁵⁻¹⁸ If the targeted application does not require the growth of thick layers, there is no reason to restrict the composition of the AlGaInP barrier to strain-free materials, even if this implies an increased complexity of the structure. Some experimental attempts on heterostructures involving strained AlGaInP might be scarcely found in literature.¹⁹⁻²⁴ Most of these deal with the strained ternary $\text{Ga}_y\text{In}_{1-y}\text{P}$,¹⁹⁻²² but lead to rather scattered results. Only one study presents measurements of the band offsets on the strained ternary $\text{Al}_x\text{In}_{1-x}\text{P}$.²³ On the other hand, a few general models have been developed, with the aim to predict the band offsets in strained heterostructures from a set of calculated or measured parameters.²⁵⁻²⁸ If these models differ on their calculation principle, they all end up by defining an energy reference level and deformation potentials.^{25,26,28} For example, Van de Walle has published²⁶ a model solid theory and calculated all the relevant parameters for most III-V compounds of interest. Since this model²⁶ does not require any further tricky calculations, it

might be used to evaluate the CBO in a first step, but a detailed comparison with experimental measurements is obviously required.

The initial goal of this study was to find the AlGaInP quaternary, eventually strained, with the highest possible conduction band minima. For that purpose, it has been decided to measure and to compare the CBO in AlGaInP/ $\text{Ga}_{0.52}\text{In}_{0.48}\text{P}$ heterostructures. The CBO in other related heterostructures, such as AlGaInP/GaAs or AlGaInP/ $\text{In}_{0.2}\text{Ga}_{0.8}\text{As}$, might be calculated from the measurements presented here and others published in literature,³ assuming transitivity. These measurements have also been fitted with calculations performed using the different set of parameters already published.²⁵⁻²⁷

This article is organized as follows. The experimental conditions are detailed in Sec. II. Heterostructures have been grown by gas-source molecular-beam epitaxy and characterized by photoluminescence (PL) and photoluminescence excitation (PLE) spectroscopy. The principle of measurement of the CBO is described in Sec. III. It involves PL and PLE measurements, aimed at determining the Γ or X character of the lower conduction state in heterostructures, while varying the well thickness (type I or II transitions). Three sets of samples have been studied, involving either the lattice-matched quaternary $(\text{Al}_z\text{Ga}_{1-z})_{0.52}\text{In}_{0.48}\text{P}$, the strained ternary $\text{Al}_x\text{In}_{1-x}\text{P}$, and quaternary $\text{Al}_{4x}\text{Ga}_x\text{In}_{1-5x}\text{P}$. All the measurements are presented and discussed in Sec. IV. It is concluded that, within the usable strain range studied here, the highest CBO is obtained for the strain-free material $\text{Al}_{0.24}\text{Ga}_{0.28}\text{In}_{0.48}\text{P}$: the expected increase of the CBO in the strained quaternary does not show up. Although it cannot be claimed that the parameters required to evaluate the CBO have been precisely determined, some improvements are obvious. First, the $E_{v,av}$ numerical parameters, initially calculated by Van de Walle²⁶ have been corrected for GaP and AlP to fit the CBO measured in strain-free materials. Second, a

^{a)}Electronic mail: dominique.vignaud@univ-lille1.fr

$\text{Al}_x\text{Ga}_{1-x}\text{In}_{1-y}\text{P}$	B
$\text{Ga}_{0.52}\text{In}_{0.48}\text{P}$	W
$\text{Al}_x\text{Ga}_y\text{In}_{1-x-y}\text{P}$	B
$\text{Ga}_{0.52}\text{In}_{0.48}\text{P}$	W

GaAs substrate and buffer

FIG. 1. Scheme of a typical heterostructure.

set of deformation potentials, related to the strain-induced displacement of the X minima, is proposed for the three binaries InP, GaP, and AlP.

II. EPITAXIAL GROWTH AND LUMINESCENCE DETAILS

Heterostructures have been grown by gas-source molecular-beam epitaxy in a Riber 32P system on GaAs (001) substrates. The growth temperature was 520 °C, as estimated by pyrometer measurements. Arsine and phosphine were thermally cracked in the same injector cell, whereas the III elements were obtained from effusion cells (two In sources). Reflection high energy electron diffraction oscillations were recorded on InP and GaAs to adjust the fluxes of III atoms. The alloy compositions and the layer thicknesses were deduced from these measurements. All epilayers were not intentionally doped. Figure 1 shows a typical sample. After the GaAs buffer, a thick $\text{Ga}_{0.52}\text{In}_{0.48}\text{P}$ layer is grown lattice matched on GaAs. It is used as a check for the composition of the well material (W) and also to absorb any residual As. The upper layers are the active ones: AlGaInP barrier layers (B) surround a thin $\text{Ga}_{0.52}\text{In}_{0.48}\text{P}$ well. By measuring heterostructures with one single V element (P) throughout the main layers, As–P intermixing problems at the interfaces are avoided. Segregation of elements III must also be considered, since it should introduce composition gradients at the interface. Because of the growth temperature, In segregation might only be a problem:^{29,30} a 1 monolayer (ML) thick In-rich layer is expected to remain at the surface during the growth of In-containing layers.²⁹ But, since the In content of all the active layers stands in the limited range $30 \leq [\text{In}] \leq 60\%$, segregation is not expected to significantly alter the alloy composition at the interfaces, and should thus be neglected. Some heterostructures have been grown with up to three thin wells with decreasing thicknesses toward the surface, in the 1–7 nm range. In some cases, the well material was $\text{Al}_{0.16}\text{Ga}_{0.36}\text{In}_{0.52}\text{P}$, always lattice matched on GaAs. Barrier materials either lattice matched on GaAs or strained (in compression or tension) have been studied, with the only restriction that the absolute value of the lattice mismatch was lower than 1%. The calculated critical thickness for lattice-mismatch relaxation by dislocations thus stands in the range 10–15 nm, at least:³¹ strained pseudomorphic barrier layers up to 10 nm thick might be grown safely without any relaxation.

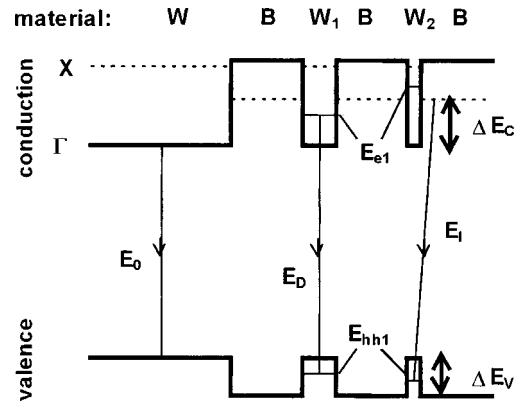


FIG. 2. Energy band extrema and luminescence transitions in an imaginary heterostructure including one thick (W) and two thin (W1 and W2) wells, all three lattice matched, surrounded by strained barriers (B). E_{e1} and E_{hh1} are the electron and heavy holes fundamental energy levels in the wells.

The PL spectra were measured at 10 K in a closed-cycle cryostat. An argon laser was used at a wavelength of 488 nm, with power fluxes in the 1–100 W/cm² range. The luminescence was dispersed in a 32 cm focal length monochromator and detected by a photomultiplier tube. PLE measurements were carried out with a 150 W Xe arc lamp combined with a double 10 cm focal length monochromator, giving power fluxes in the 1–10 mW/cm².

III. CONDUCTION BAND OFFSET MEASUREMENTS

A. Measurement principle

An imaginary heterostructure is schematized in Fig. 2 to explain the principle of the determination of the CBO. This method was already used to measure the CBO in AlAs/GaAs (Ref. 32) as well as $(\text{Al}_z\text{Ga}_{1-z})_{0.52}\text{In}_{0.48}\text{P}/\text{Ga}_{0.52}\text{In}_{0.48}\text{P}$ heterostructures.^{11,12} It involves one thick and two thin wells W1 and W2, all made of the same material W. The thicknesses of the latter two are chosen to obtain an electron quantized level lower than the X state of the barrier (B) in one well (W1) and higher in the thinner one (W2). Three radiative recombinations are expected in this case. By order of increasing energy, they are labeled E_0 , E_D and E_I in Fig. 2. Transitions in the thick well, typical of the band gap in the “bulk” material W, occur at the lower-energy E_0 . The PL peak E_D involves direct recombinations (type I) of electrons and holes in the well W1. Since the Γ electron energy level is higher in the “well” W2 than the X energy level in the surrounding “barriers,” the electrons created inside W2 first thermalize to the X state in the barriers: this leads to the type II luminescence at E_I , which is indirect in both real and reciprocal spaces. The conduction band offset ΔE_c between the X state in the barrier and the Γ state in the material W is thus given by (see Fig. 2):

$$\Delta E_c = E_I - E_0 - E_{hh1} \quad (1)$$

where E_{hh1} is the confining energy of the heavy holes, calculated in the thinner well W2. It mainly depends on the well thickness, which is known from the growth parameters, but also on the valence band offset (VBO) ΔE_v between the barrier and well materials. Since the sum of the CBO and

VBO is equal to the band gap difference, the problem should be solved self-consistently if the indirect band gap of the barrier is accurately known. When this is not the case, noticeably for strained quaternary materials, one must rely on an estimated value of ΔE_v , resulting in an increased error on the experimentally determined ΔE_c . Fortunately, E_{hh1} is a slowly varying function of the VBO, because of the large mass of the heavy holes. It has been checked in a few cases with lattice-matched barriers that the value of ΔE_c obtained from an estimated ΔE_v is close to the one calculated when the full self-consistent problem is solved. Formally, the PL peak energies which appear in Eq. (1) should be corrected for the exciton energy. Since both corrections are small, and since this equation involves the difference $E_I - E_0$, the as-measured values have been directly used. One restriction of this method should be pointed out: only CBO between an X state in the barrier and a Γ state in the well can be directly determined. But, it is far more sensitive on the CBO than the method of fitting the direct PL transition energies in wells of different thickness with calculations, as already pointed out.^{33,34} All the material parameters required in the calculations are the one given in the recent review by Vurgaftman *et al.*,³ with the exception of the average valence band and of the deformation potentials which have been taken from Ref. 26 (see the reminder on the model solid theory in Sec. IV A). Ternary and quaternary parameters have been linearly interpolated between the corresponding ones of the related binaries, with the exception of the direct and indirect band gaps for which quadratic laws have been used, following Ref. 3.

B. Direct/indirect transition identification

The method described in the preceeding paragraph critically relies on the identification of the direct or indirect character of PL bands. This has been achieved through two different and complementary approaches. Both methods were systematically used for all the samples presented here. The first one exploits the fact that indirect transitions should be far less efficient than direct ones. This is illustrated in Fig. 3, which shows the PL spectra measured on two heterostructures identical to the typical one schematized in Fig. 1, with $\text{Al}_{0.46}\text{In}_{0.54}\text{P}$ barriers. The only difference between both heterostructures is the thin well thickness, which is, respectively, 3 and 4 (MLs). In the 3 ML sample, the thin well PL is more than one order of magnitude less intense than in the 4 ML sample, and slightly shifted toward higher energies (2.258 eV and 2.242 eV, respectively). At the same time, the PL from the thick wells ($\text{Ga}_{0.52}\text{In}_{0.48}\text{P}$ reference) present almost identical peak energies (1.954 and 1.956 eV) as well as intensities for both heterostructures. These observations are fully consistent with an indirect transition in the 3 ML sample and a direct one in the 4 ML sample. The slight energy shift between the thin well PL comes from the increase of the confinement energy of the heavy holes when the well thickness is reduced. With an estimated $\Delta E_v = 250$ meV, one calculates $E_{hh1} = 160$ meV which gives a CBO $\Delta E_c = 145 \pm 30$ meV for the heterostructure $\text{Al}_{0.46}\text{In}_{0.54}\text{P}/\text{Ga}_{0.52}\text{In}_{0.48}\text{P}$.

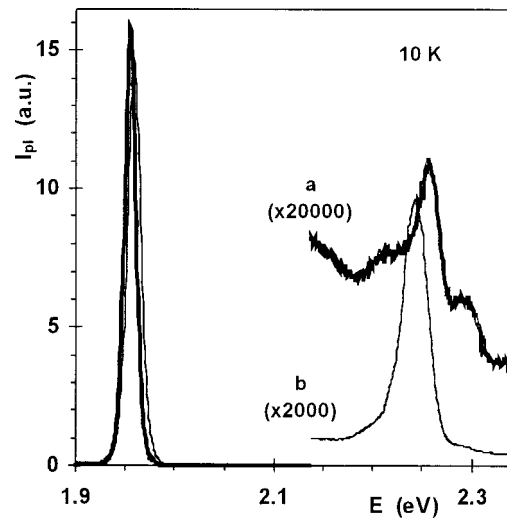


FIG. 3. PL spectra measured in two almost identical heterostructures, each including one 150 nm thick and one thin [3 MLs (a) or 4 MLs (b)] $\text{Ga}_{0.52}\text{In}_{0.48}\text{P}$ wells surrounded by compressively strained $\text{Al}_{0.46}\text{In}_{0.54}\text{P}$ barriers.

The first approach based on the PL intensity was not always conclusive, because the intensity drop obtained while reducing the well thickness was too low. In such cases, transition identification might nevertheless be achieved through the study of the PLE spectra. Figure 4 illustrates this method, with luminescence measurements obtained with an heterostructure including three thin wells, respectively, 7, 5, and 2 nm thick with $\text{Al}_{0.6}\text{In}_{0.4}\text{P}$ barriers. The three corresponding PL peaks are located at 2.014, 2.061, and 2.129 eV. The threshold of PLE is shifted by 140 meV toward higher energy compared to the corresponding PL peak for the thinner well (see curve c in Fig. 4), which is characteristic of an indirect PL transition in the reciprocal space. On the contrary, there is no shift between the PLE and PL spectra in the 7 and 5 nm wells (see curves a and b in Fig. 4). The transi-

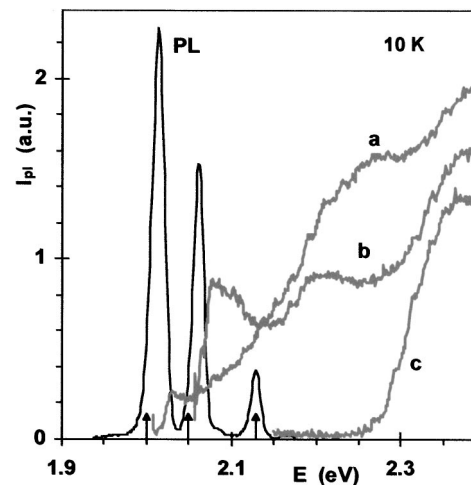


FIG. 4. PL (thin line) measured in an heterostructure, including three $\text{Ga}_{0.52}\text{In}_{0.48}\text{P}$ wells (7, 5, and 2 nm thick) surrounded by compressively strained $\text{Al}_{0.46}\text{In}_{0.54}\text{P}$ barriers. The arrows indicate the energy at which the corresponding PLE spectra (labeled a, b, and c, thick lines) have been recorded.

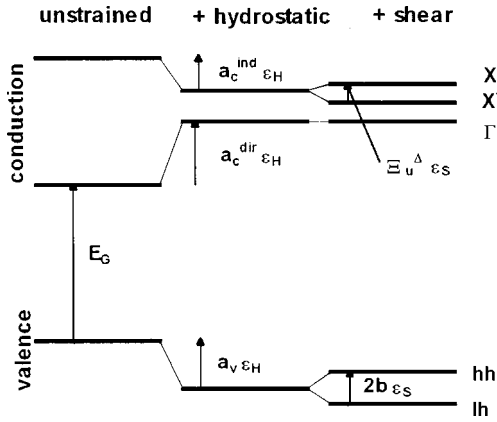


FIG. 5. Scheme of the strain induced changes of the band structure, limited to the Γ and X conduction band minima and light and heavy holes valence band maxima. From the left- to right-hand side, the extrema are shown unstrained, then submitted to an hydrostatic strain, then with a shear strain added (corresponding to the full pseudomorphic case).

tions are direct in the reciprocal space, which means that the minimum conduction energy level remains a Γ state in the two $\text{Ga}_{0.52}\text{In}_{0.48}\text{P}$ thicker wells.

IV. CONDUCTION BAND OFFSETS: RESULTS AND DISCUSSION

A. Reminder: Model solid theory

This model has been developed by Van de Walle with the aim to predict band offsets at both lattice-matched and strained interfaces.²⁶ The relative alignment of the valence bands of different strain-free materials is described by one single parameter for each, called $E_{v,av}$. Its meaning is the average of the three valence band maxima (heavy and light holes, spin-orbit split-off band) relative to a common reference level. Calculated values of $E_{v,av}$ have been published, and appear to predict band offsets consistent with experimental measurements.²⁶ When a strain is added, the displacement of the bands relative to the unstrained case is measured by deformation potentials. One parameter is required for each band at each extrema for the hydrostatic component of the strain. Furthermore, additional parameters are needed to describe the splitting of the degenerated levels induced by the shear part of the pseudomorphic strain. This is schematized in Fig. 5. In the case of interest here, the heavy and light hole bands (valence band) and the Γ and X bands (conduction band) are only considered. For the sake of simplicity, the L minima of the conduction band and the split-off valence band are not drawn. This means that three hydrostatic deformation potentials, a_c^{dir} , a_v , and a_c^{ind} , and two shear deformation potentials, b and Ξ_u^{Δ} , are involved (following the notation of Ref. 26). If most of these parameters have been calculated by Van de Walle²⁶ for the materials concerned here, the X shear deformation potential is missing. Furthermore, other calculations of the same deformation potentials a_c^{dir} , a_v , and a_c^{ind} gave somewhat different values:^{25–27} for example, a_v is always positive²⁶ or negative,²⁵ whereas both signs are found in Ref. 27. A direct comparison with experiments is not an easy task, since these parameters are not all experimentally measurable. For example, the hydrostatic

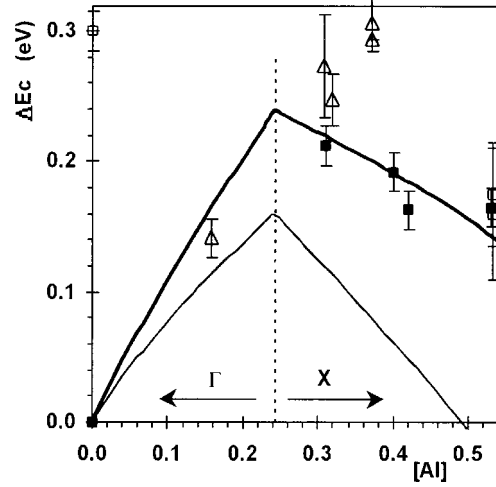


FIG. 6. The measured conduction band offset in $(\text{Al}_z\text{Ga}_{1-z})_{0.52}\text{In}_{0.48}\text{P}/\text{Ga}_{0.52}\text{In}_{0.48}\text{P}$ heterostructures lattice matched on GaAs (filled squares). Data from literature (Refs. 4–12) are also shown for comparison: this includes the Γ – Γ (empty triangles) and the X – Γ offsets (empty squares). Continuous lines are calculations based on the model solid theory, with $E_{v,av}(\text{AIP}) = -8.09$ eV (thin line) or $E_{v,av}(\text{AIP}) = -7.77$ eV (thick line). The Γ or X character of the conduction band minimum of the barrier is also indicated.

pressure induced changes of the band gaps (direct or indirect) have been determined, which gives values for $a_c^{\text{dir}} - a_v$ and $a_c^{\text{ind}} - a_v$ if the bulk modulus is known. But, no accurate measurements of the relative changes of each band can be carried out. As for the shear deformation potentials, the value of b , which is a measure of the splitting of the heavy and light hole bands, is available for all three binaries InP, GaP, and AlP.³ On the contrary, measurements related to the splitting of the X minima Ξ_u^{Δ} are rather uncommon. Values in the range 5–7 eV have been mentioned for GaAs, GaP, and AlAs.^{35,36} Calculations of Ξ_u^{Δ} are even more scarce, with only one work giving numerical values for two III–V compounds only,²⁶ 8.6 eV in GaAs and 4.5 eV for InAs. From these limited data, one might only assume that Ξ_u^{Δ} should be positive for any III–V compound, in the range 4–10 eV.

B. Lattice-matched $(\text{Al}_z\text{Ga}_{1-z})_{0.52}\text{In}_{0.48}\text{P}/\text{Ga}_{0.52}\text{In}_{0.48}\text{P}$ heterostructures

CBO measurements have been first carried out on a set of lattice-matched $(\text{Al}_z\text{Ga}_{1-z})_{0.52}\text{In}_{0.48}\text{P}/\text{Ga}_{0.52}\text{In}_{0.48}\text{P}$ heterostructures. The goal was to validate the method by comparison with data published in literature,^{4–12} obtained after PL experiments combined with either hydrostatic pressures^{4–8} or PLE.^{9–11} It was also aimed at determining the maximum CBO in the lattice-matched case. The measurements are drawn in Fig. 6, together with previously published data.^{4–12} The largest measured offset is 210 ± 15 meV for the $\text{Al}_{0.31}\text{Ga}_{0.21}\text{In}_{0.48}\text{P}/\text{Ga}_{0.52}\text{In}_{0.48}\text{P}$ heterostructure, which reasonably fits previously measured data also shown in Fig. 6. Calculations of the band offset using the set of parameters computed by Van de Walle²⁶ are also drawn in Fig. 6 (thin line). They obviously underestimate the CBO. Because these calculations are related to unstrained materials, the only relevant parameter which might be adjusted is $E_{v,av}$ for each of

TABLE I. The parameters used for the calculations of the conduction band offset based on the model solid theory.

	$E_{v,av}$	a_c^{ind}	Ξ_u^Δ
InP	-7.04 ^a	3.5 ^{a,c}	6 ^b
GaP	-7.56 ^b	3.26 ^a	6.5 ^d
AlP	-7.92 ^b	5.12 ^a	6 ^b

^aSee reference 26.^bThis work.^cValue obtained using the experimentally measured $a_c^{ind} - a_v = 2.2$ eV (Ref. 39) and the calculated a_v of Ref. 26.^dSee reference 35.

the three binaries involved. Furthermore, since the [In] content is almost constant on both sides of lattice-matched $(Al_xGa_{1-x})_{0.52}In_{0.48}P/Ga_{0.52}In_{0.48}P$ heterostructures, the fit cannot be significantly improved by modifying $E_{v,av}$ for the binary InP. Figure 6 shows the best fit of the CBO with a thick line, using $E_{v,av}(AlP) = -7.77$ eV instead of -8.09 eV.²⁶ An opposite change of $E_{v,av}(GaP)$ (-7.74 eV instead of -7.4 eV²⁶), or an appropriate combination of both would have led to the same curve. Furthermore, if one takes into account the VBO of 0.6 eV deduced after measurements in GaP/InP strained-layer superlattices,³⁷ the problem now has an unique solution: one obtains $E_{v,av}(AlP) = -7.92$ eV and $E_{v,av}(GaP) = -7.56$ eV (see Table I). The largest calculated CBO is found for the $Al_{0.24}Ga_{0.28}In_{0.48}P$ material, for which the Γ and X states are degenerate. This composition agrees with previously published measurements,¹⁵⁻¹⁸ within experimental errors. Let us finally mention that with the numerical values of $E_{v,av}$ mentioned herein, one finds a VBO of 0.36 eV for the AlP/GaP heterostructure. This is in better agreement with experiments³⁸ ($\Delta E_v = 0.43$ eV) than the one calculated from the initial parameters of Ref. 26 (leading to $\Delta E_v = 0.69$ V).

C. Strained $Al_xIn_{1-x}P/Ga_{0.52}In_{0.48}P$ and $AlGaInP/Ga_{0.52}In_{0.48}P$ heterostructures

A first set of strained heterostructures have been studied, with the ternary $Al_xIn_{1-x}P$ as the barrier material. Both compressive and tensile strained layers have been measured, the results of which being shown in Fig. 7. Previously published data, measured over a smaller composition range, are also shown in this Fig. 7: both sets of measurements agree. The maximum CBO is found for the lattice-matched composition, although all the measured values on the compressive side (with $0.4 \leq [Al] \leq 0.53$) are almost identical within experimental errors. A change of slope of the CBO versus [Al] content on both sides of the lattice-matched composition is obvious. This implies that the X -band six-fold degeneracy is partially raised by the shear part of the strain (compare to the thin line in Fig. 7, for which Ξ_u^Δ was set equal to 0 for all binaries, see also Fig. 5). Figure 7 also shows the calculated CBO for different set of parameters. Assuming that the values of $E_{v,av}$ are determined after the measurements on strain-free heterostructures, the relevant parameters in this case are the X -band related deformation potentials a_c^{ind} and Ξ_u^Δ for the binaries AlP and InP. A first set of a_c^{ind} has been used (see Table I), as calculated by Van de Walle.²⁶ It leads to a good

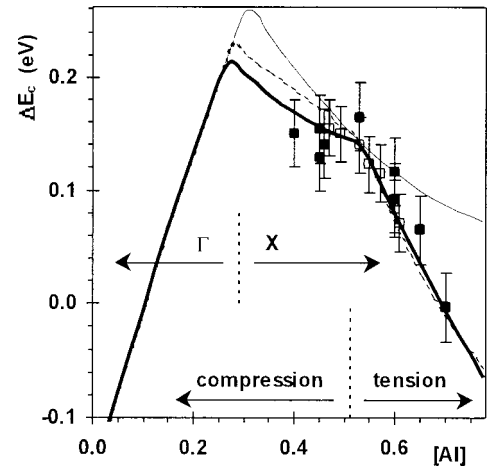


FIG. 7. The measured conduction band offset in $Al_xIn_{1-x}P/Ga_{0.52}In_{0.48}P$ heterostructures (filled squares). Data from literature (see Ref. 23) are also shown for comparison (empty squares). Lines are calculations based on the model solid theory, using the a_c^{ind} deformation potentials [from Ref. 26 (continuous lines) or Ref. 25 (dashed line)], with $\Xi_u^\Delta = 0$ (thin line) or 6 eV (thick line).

fit with the experimental data, assuming $\Xi_u^\Delta = 6$ eV for both binaries AlP and InP (a value consistent with the rare determinations of this deformation potential in other III-V compounds.^{35,36} Using identical values of Ξ_u^Δ for both InP and AlP is a simplification, but only measurements on each binary would allow an accurate fit for each material. On the contrary, the sets of deformation potentials calculated in Refs. 25 or 27 give less satisfactory fits, since they compel one to use unexpectedly high ($\Xi_u^\Delta = 12$ eV for InP) and low ($\Xi_u^\Delta = 0$ eV for AlP) values (see the dashed line in Fig. 7). This discrepancy appears to come mainly from the low value of a_c^{ind} and a_v calculated in both Refs. 25 and 27 for InP. So, the solution of the CBO problem in terms of Van de Walle's model,²⁶ combined with the numerical parameters gathered in Table I, agrees well with the limited set of experimental results shown here.

A third set of samples, characterized by compressively strained barriers with $[Al]/[Ga] = 4$, has been also studied. This particular range of composition of the barriers has been chosen because initial simulations with a "reasonable" set of parameters showed that large CBO could be expected in this range. The corresponding CBO, not shown here, leads to the conclusion similar to the one reached after measurements on $Al_xIn_{1-x}P/Ga_{0.52}In_{0.48}P$ heterostructures. Once again, the maximum CBO measured is for the lattice-matched heterostructure ($Al_{0.42}Ga_{0.11}In_{0.47}P/Ga_{0.52}In_{0.48}P$): a significant increase of the CBO cannot be achieved in such compressively strained layers in comparison to the strain-free case.

Even if the deformation potentials could not be precisely fitted by the measurements presented here, the set of parameters gathered in Table I can be used to extrapolate the CBO for any $AlGaInP/Ga_{0.52}In_{0.48}P$ heterostructure. The error made obviously grows as the strain increases, since uncertainties remain mainly on the strain-related corrections. But it seems significant that the evaluated CBO never exceeds the one calculated for the lattice-matched barriers. Notice-

ably, the large value of the X-band splitting deformation potentials Ξ_u^A seems responsible for this effect. So, the initial assumption that the CBO might be increased by the strain is not confirmed.

V. CONCLUSIONS

The CBO has been measured in strain-free, compressively, and tensile-strained AlGaInP/Ga_{0.52}In_{0.48}P heterostructures, by combined PL–PLE experiments. A maximum CBO of 210 ± 15 meV has been found for the barrier Al_{0.31}Ga_{0.21}In_{0.48}P, lattice matched on GaAs. Assuming transitivity of the band offsets and a CBO of 180 meV for the heterostructure Ga_{0.52}In_{0.48}P/GaAs,³ the maximum CBO at the AlGaInP/GaAs is 390 meV: this is significantly larger than the highest CBO in the AlGaAs/GaAs system of 300 meV.³ None of the strained AlGaInP/Ga_{0.52}In_{0.48}P heterostructures has shown a measured CBO larger than 210 meV. Fitting this limited set of experimental results with the model solid theory leads to an improvement of the $E_{v,av}$ parameters initially calculated in Ref. 26. Although the deformation potentials required to model the full problem could not be precisely adjusted, approximate calculations combined with those measurements suggest that one reject the assumption that the CBO could be increased by using strained quaternary layers AlGaInP.

ACKNOWLEDGMENT

The authors are indebted to C. Coinon for help with the molecular-beam epitaxy growth.

¹J. M. Kuo, Thin Solid Films **231**, 158 (1993).

²J. Dickmann, M. Berg, A. Geyer, H. Dämbkes, F. Scholz, and M. Moser, IEEE Trans. Electron Devices **42**, 2 (1995).

³I. Vurgaftman, J.R. Meyer, and L.R. Ram-Mohan, J. Appl. Phys. **89**, 5815 (2001).

⁴D. Patel, M.J. Hafich, G.Y. Robinson, and C.S. Menoni, Phys. Rev. B **48**, 18031 (1993).

⁵M.D. Dawson, S.P. Najda, A.H. Kean, G. Duggan, D.J. Mowbray, O.P. Kowalski, M.S. Skolnick, and M. Hopkinson, Phys. Rev. B **50**, 11190 (1994).

⁶A.D. Prins, J.L. Sly, A.T. Meney, D.J. Dunstan, E.P. O'Reilly, A.R. Adams, and A. Valster, J. Phys. Chem. Solids **56**, 423 (1995).

⁷A.T. Meney, A.D. Prins, A.F. Phillips, J.L. Sly, E.P. O'Reilly, D.J. Dunstan, A.R. Adams, and A. Valster, IEEE J. Sel. Top. Quantum Electron. **1**, 697 (1995).

⁸J.W. Cockburn, O.P. Kowalski, D.J. Mowbray, M.S. Skolnick, R. Teissier, and M. Hopkinson, *Proceedings of the 22nd International Conference Phys. of Semiconductors* (Vancouver 1994) (World Scientific, Singapore, 1995), p. 747.

⁹C.T.H.F. Liedenbaum, A. Valster, A.L.G.J. Severens, and G.W. 't Hooft, Appl. Phys. Lett. **57**, 2698 (1990).

¹⁰M.D. Dawson and G. Duggan, Phys. Rev. B **47**, 12598 (1993).

¹¹Y. Ishitani, S. Minagawa, T. Kita, T. Nishino, H. Yaguchi, and Y. Shiraki, J. Appl. Phys. **80**, 4592 (1996).

¹²J.D. Lambkin, A.P. Morrison, L. Considine, G.M. O'Connor, C.J. McDonagh, E. Daly, and T.J. Glynn, *Proceedings of the 22nd International Conference Phys. of Semiconductors* (Vancouver 1994) (World Scientific, Singapore, 1995), p. 707.

¹³M.J. Jou, J.F. Lin, C.M. Chang, C.H. Lin, M.C. Wu, and B.J. Lee, Jpn. J. Appl. Phys., Part 1 **32**, 4460 (1993).

¹⁴H. K. Yow, P. A. Houston, and M. Hopkinson, Appl. Phys. Lett. **66**, 2852 (1995).

¹⁵D. J. Mowbray, O. P. Kowalski, M. Hopkinson, M. S. Skolnick, and J. P. R. David, Appl. Phys. Lett. **65**, 213 (1994).

¹⁶J. S. Nelson, E. D. Jones, S. M. Myers, D. M. Follstaedt, H. P. Hjalmarson, J. E. Schirber, R. P. Schneider, J. E. Fouquet, V. M. Robbins, and K. W. Carey, Phys. Rev. B **53**, 15893 (1996).

¹⁷U. Dör, W. Schwarz, A. Wörner, R. Westphäling, A. Dinger, H. Kalt, D. J. Mowbray, M. Hopkinson, and W. Langbein, J. Appl. Phys. **83**, 2241 (1998).

¹⁸X. H. Zhang, S. J. Chua, and W. J. Fan, Appl. Phys. Lett. **73**, 1098 (1998).

¹⁹T. Y. Wang, A. W. Kinball, G. S. Chen, D. Birkedal, and G. B. Stringfellow, J. Appl. Phys. **68**, 3356 (1990).

²⁰K. Interholzinger, D. Patel, C. S. Menoni, P. Thiagarajan, G. Y. Robinson, and J. E. Fouquet, IEEE J. Quantum Electron. **34**, 93 (1998).

²¹T. M. Ritter, B. A. Weinstein, R. E. Viturro, and D. P. Bour, Phys. Status Solidi B **211**, 869 (1999).

²²J. Martinez-Pastor, J. Camacho, C. Rudamas, A. Cantarero, L. Gonzalez, and K. Syassen, Phys. Status Solidi A **178**, 571 (2000).

²³Y. Ishitani, E. Nomoto, T. Tanaka, and S. Minagawa, J. Appl. Phys. **81**, 1763 (1997).

²⁴S. J. Chang and C. S. Chang, IEEE Photonics Technol. Lett. **10**, 651 (1998).

²⁵M. Cardona and N. E. Christensen, Phys. Rev. B **35**, 6182 (1987).

²⁶C. G. Van de Walle, Phys. Rev. B **39**, 1871 (1989).

²⁷S. H. Wei and A. Zunger, Phys. Rev. B **60**, 5404 (1999).

²⁸C. Ohler, C. Daniels, A. Förster, and H. Lüth, Phys. Rev. B **58**, 7864 (1998).

²⁹J. M. Moison, C. Guille, F. Houzay, F. Barthe, and M. Van Rompay, Phys. Rev. B **40**, 6149 (1989).

³⁰O. Dehaese, X. Wallart, and F. Mollot, Appl. Phys. Lett. **66**, 52 (1995).

³¹E. A. Fitzgerald, Mater. Sci. Rep. **7**, 87 (1991).

³²G. Danan, B. Etienne, F. Mollot, R. Planel, A. M. Jean-Louis, F. Alexandre, B. Jusserand, G. Le Roux, J. Y. Marzin, H. Savary, and B. Sermage, Phys. Rev. B **35**, 6207 (1987).

³³R. P. Schneider, R. P. Bryan, E. D. Jones, and J. A. Lott, Appl. Phys. Lett. **63**, 1240 (1993).

³⁴D. J. Mowbray, O. P. Kowalski, M. S. Skolnick, M. Hopkinson, and J. P. R. David, Superlattices Microstruct. **15**, 313 (1994).

³⁵Landolt-Börnstein, *Numerical Data and Functional Relationships in Science and Technology*, New Series, III/Vol. 17a, edited by O. Madelung, M. Schultz, and H. Weiss (Springer, Berlin, 1982).

³⁶P. Lefebvre, B. Gil, H. Mathieu, and R. Planel, Phys. Rev. B **40**, 7802 (1989).

³⁷G. Armeles, M. C. Munoz, and M. I. Alonso, Phys. Rev. B **47**, 16299 (1993).

³⁸J. R. Waldrop, R. W. Grant, and E. A. Kraut, J. Vac. Sci. Technol. B **11**, 1617 (1993).

³⁹H. Müller, R. Trommer, M. Cardona, and P. Vogl, Phys. Rev. B **21**, 4879 (1980).